

論文 / 著書情報  
Article / Book Information

Title	Silicon Nanoparticles Prepared by Laser Ablation in Electolyte Solution
Authors	Pattarin Chewchinda, Osamu Odawara, Hiroyuki Wada
Citation	CheM, Vol. 3, , p. 81-86
Pub. date	2016, 1

**Title:** Silicon Nanoparticles Prepared by Laser Ablation in Electrolyte Solution

**Authors:** Pattarin Chewchinda, Osamu Odawara and Hiroyuki Wada

**Affiliation:** Department of Innovative and Engineered Materials, Tokyo Institute of Technology,  
4259 Nagatsuta-cho, Midori, Yokohama, Kanagawa 226-8503, Japan

**Corresponding author:**

Hiroyuki Wada (Prof. / Ph.D.)

E-mail: wada.h.ac@m.titech.ac.jp

Postal address: 4259 Nagatsuta, #J2-41, Midori-ku, Yokohama 226-8502 Japan

Phone/Fax: +81 45 924 5362

**Abstract:**

In this study, silicon nanoparticles are prepared by laser ablation in electrolyte solution (NaCl, NaBr, and NaI). Particle stability was decreased as NaCl concentration increases, while the particles prepared in NaBr and NaI remained stable. From TEM images, well-dispersed spherical particles were obtained. However, as NaCl concentration exceeded 6 mM, particle aggregation was observed. Raman spectra verified that small crystalline particles were prepared in all samples with no trace of amorphous structure. Depending on polarizability, ions adsorbed onto the particle surface at different affinity. Since the polarizability of Cl ion is low, it loosely attached to the particle surface leading to an inefficient charge transfer. As electrolyte concentration increased, electric double layer became thinner and the particle surface charge was insufficient for electrostatic repulsion. Consequently, attractive potential became dominant leading to particle aggregation.

**Keywords:** laser ablation, silicon, electrolyte, nanoparticles, colloid

**Introduction**

The discovery of quantum dots or nanoparticles has raised expectations in advanced biological research. Compared to conventional organic fluorophores, inorganic nanoparticles offer longer fluorescence lifetime. As a consequence, these particles are easily distinguishable from other fluorophores and background [1-3]. Besides, their optical properties are size-dependent [4-6]. They can be simultaneously excited by a single wavelength but emit different colors. This property provides them as an ideal probe for multicolor experiment [2, 7-8]. In addition, inorganic nanoparticles possess sufficient photostability and high resistance to metabolic degradation [2, 8-9]. According to these reasons, inorganic nanoparticles are a potential candidate for a substitution of unstable organic fluorophores.

In order to utilize these particles in biological application, an issue regarding toxicity is a major concern. Although recent development of II-IV nanoparticles such as CdSe and CdS shows their excellent stability and high fluorescence, their cytotoxicity is still concerned. Thus, their applications in bio-related field are limited [10].

Silicon (Si) nanoparticles offer a better alternative as a fluorescence probe owing to their non-toxicity. Erogbogbo *et al.* prepared silicon nanoparticles using polyethyleneglycol (PEG) phospholipids micelles [11]. These particles were characterized in biologically related conditions and they were found to be stable. To study *in vitro* cell-labeling, Si nanoparticles were integrated in a human pancreatic cancer cell and a strong optical signal was detected with no observable toxicity. They also applied these particles for *in vivo* multicolored imaging experiment [7]. The luminescence from these particles was easily differentiated from the background, which verified their potential as a multicolored optical probe. Li *et al.* reported that poly(acrylic acid) grafted Si nanoparticles provided bright photoluminescence (PL) and had better resistance against photo-bleaching compared to organic dyes [12]. Wang *et al.* showed that the fluorescence lifetime of Si nanoparticles was approximately two times longer than that of cellular fluorophores [1]. In addition, these particles were stable in broad pH range and their toxicity was minimum. These studies have justified the potential of Si nanoparticles in biological application.

Several attempts have been made in order to prepare Si nanoparticles. Among them, laser ablation in liquid is considered as a simple, versatile, and clean synthesis. However, it has been showed that the properties of the prepared particles strongly depend on experimental parameters [13-24]. Since inorganic salts are one of the main substances in biological systems, a study on ions and nanoparticles interaction is important. In this work, Si nanoparticles are prepared by laser ablation in electrolyte solution including NaCl, NaBr, and NaI. The effect of ions and electrolyte concentration on the prepared Si nanoparticles are studied and compared.

## **Experiment**

Q-switch Nd:YAG laser (532 nm, 10 Hz, 13 ns) was employed as an irradiation source with energy density of 0.4 J/cm<sup>2</sup>. P-type silicon wafer (resistivity 11.5-15.5 Ω·cm, thickness 600 μm, dimension 2x2 cm) was immersed in 15 mL of electrolyte solution (NaCl, NaBr, or NaI) with concentration varied from 2 to 10 mM. The target was irradiated for 30 minutes. The prepared colloidal solution was transferred into disposable capillary cell (DTS1070) and zeta potential was measured with Malvern Zetasizer Nano ZS. Transmission Electron Microscope (Hitachi H-8100 TEM, 200 kV) was employed to observe particle size and morphology. Energy Dispersive X-ray Spectroscopy (EDS) point analysis was operated by Field Emission Transmission Electron Microscope (JEM 2010F, 200 kV) to confirm the composition of the synthesized particles. From these images, particle size distributions were constructed by measuring the diameter of 500 nanoparticles with ImageJ software. These results were fitted with lognormal distribution by OriginPro 9.0 software. Raman spectra were collected at room temperature with Ar<sup>+</sup> laser (514.5 nm, 50 mW).

## **Results and discussion**

Fig. 1 shows TEM images of the samples prepared in NaCl solution along with their size distribution. From these results, well-dispersed spherical particles are obtained in the concentration range of 2 to 6 mM. In addition, the majority of particles are smaller than 10 nm. However, as the concentration increases further to 8 mM, particles start to interact and small aggregates are observed. After reaching 10 mM, severe aggregation occurs and the number of large particles beyond 10 nm increases. EDS result shown in Fig. 2 confirms the adsorption of Cl on the particle surface. The detected oxygen peak indicates that surface oxidation possibly occurs in the sample. Particle stability can be determined by zeta potential measurement. The absolute value of zeta potential tends to decrease as NaCl concentration increases. This result suggests that the particle stability decreases with an increase in NaCl concentration.

For the samples prepared in NaBr and NaI solution, spherical particles are well dispersed within the experimental range. The particle size of the samples prepared in NaBr and NaI solution is smaller than 10 nm and 7 nm, respectively. Fig. 3 shows the size distribution of the samples prepared in NaBr solution along with their corresponding TEM images. For the samples prepared in NaI solution, the results are similar and shown in Appendix A.

For the samples prepared in NaCl solution, Raman peaks shift from bulk silicon ( $520\text{ cm}^{-1}$ ) to lower frequency, as shown in Fig. 4. This red shift verifies the existence of small crystalline silicon in the samples, which is further confirmed by high resolution TEM (HRTEM) image as shown in the inset of Fig. 4 [25-27]. Additionally, a broad peak centered at  $480\text{ cm}^{-1}$  is not detected indicating the absence of amorphous structure [17, 28-30]. Similar results are obtained for the samples prepared in NaBr and NaI solution, as shown in Appendix B.

Until now, the process of nanoparticles formation by laser ablation in liquid is still under debate. However, some authors believe that the particle formation occurs within the cavitation bubble [32-33]. Following this assumption, the interaction between particles and solution possibly occurs after the cavitation bubble collapsed. Subsequently, the competition between existed ions determines the surface properties of the particles.

Table 1 shows the polarizability data obtained from literatures. Since the van der Waals attraction increases with polarizability of sorbate species [36], the surface adsorption follows the order  $I^- > Br^- > Cl^- \gg Na^+$ .

Comparing between anions,  $Cl^-$  loosely adsorb on the particle surface owing to its low polarizability and the charge transfer process becomes inefficient. As electrolyte concentration increases, electric double layer thickness decreases [37]. Consequently, the attractive potential can overcome the electrostatic repulsion and particles start to interact, grow, and agglomerate. For  $Br^-$  and  $I^-$ , the adsorption and the charge transfer process on the particle surface becomes efficient. Owing to high surface charge, the electrostatic repulsion is still dominant and the particles are stabilized against further growth and agglomeration even at high electrolyte concentration. The effect of electrolyte concentration and particle surface charge on electric double layer thickness is summarized in Fig. 5. The results would be related to halogen bond (XB) which was a non-covalent bond. In this case, halogen is an electron acceptor and the bond was formed with electron donor (Lewis base) like hydrogen bond. The halogen bond is widely studied in various research field such as Liquid Crystals, drug, self-assembly, crystal engineering, and biological system [38-41]. In general, strength of the interaction indicates tendency like  $Cl < Br < I$ , which means  $I$  forms strongest halogen bond. This tendency supports our experimental results, which would be related to the usage of halogen bond interaction for nanoparticle.

## Conclusions

Silicon nanoparticles are successfully prepared by laser ablation of silicon target in electrolyte solution. The results show that an increase in  $NaCl$  solution reduces particle stability and increases particle size. For those prepared in  $NaBr$  and  $NaI$  solution, stable particles are obtained within the experimental range. In addition, good particle crystallinity was observed with no evidence of amorphous structure.

## Acknowledgments

We would like to thank Prof. Kazutaka Nakamura, Prof. Yoshitaka Kitamoto, Prof. Hiroshi Funakubo, Prof. Masahiko Hara, and Prof. Tomohiro Hayashi for their generous support in research facilities. In addition, we would like to acknowledge Mr. Katsuaki Hori for his contribution to this research. This work was supported by JSPS KAKENHI, the Collaborative Research Project of Materials & Structures Laboratory (Tokyo Tech.), and the Center for Advanced Materials Analysis (Tokyo Tech.).

## References

- [1] J. Wang, D. Ye, G. Liang, J. Chang, J. Kong, and J. Chen: *J. Mater. Chem. B*, 2, (2014) 4338.
- [2] P. Sharma, S. Brown, G. Walter, S. Santra, and B. Moudgil: *Adv. Colloid Interface Sci.*, 123-126, (2006) 471.
- [3] A. G. Cullis, L. T. Canham, and P. D. J. Calcott: *J. Appl. Phys.*, 82, (1997) 909.
- [4] N. Shirahata, D. Hirakawa, Y. Masuda, and Y. Sakka: *Langmuir*, 29, (2013) 7401.
- [5] Z. Kang, Y. Liu, C. H. A. Tsang, D. D. D. Ma, X. Fan, N. Wong, and S. Lee: *Adv. Mater.*, 21, (2009) 661.
- [6] K. Saitow, and T. Yamamura: *J. Phys. Chem. C*, 113, (2009) 8465.
- [7] F. Erogbogbo, K. Yong, I. Roy, R. Hu, W. Law, W. Zhao, H. Ding, F. Wu, R. Kumar, M. T. Swihart, and P. N. Prasad: *ACS Nano*, 5, (2011) 413.
- [8] M. A. Walling, J. A. Novak, and J. R. E. Shepard: *Int. J. Mol. Sci.*, 10, (2009) 441.
- [9] H. Arya, Z. Kaul, R. Wadhwa, K. Taira, T. Hirano, and S. C. Kaul: *Biochem. Biophys. Res. Commun.*, 329, (2005) 1173.
- [10] A. M. Derfus, W. C. W. Chan, and S. N. Bhatia: *Nano Lett.*, 4, (2004) 11.
- [11] F. Erogbogbo, K. Yong, I. Roy, G. Xu, P. N. Prasad, and M. T. Swihart: *ACS Nano*, 2, (2008) 873.

- [12] Z. F. Li, and E. Ruckenstein: *Nano Lett.*, 4, (2004) 1463.
- [13] V. Švrček, T. Sasaki, Y. Shimizu, and N. Koshizaki: *Appl. Phys. Lett.*, 89, (2006) 213113.
- [14] S. Yang, W. Cai, H. Zhang, X. Xu, and H. Zeng: *J. Phys. Chem. C*, 113, (2009) 19091.
- [15] D. Rioux, M. Laferrière, A. Douplik, D. Shah, L. Lilge, A. V. Kabashin, and M. Meunier: *J. Biomed. Opt.*, 14, (2009) 021010.
- [16] S. Besner, J.-Y. Degorce, A. V. Kabashin, and M. Meunier: *Appl. Surf. Sci.*, 247, (2005) 163.
- [17] R. Intartaglia, K. Bagga, F. Brandi, G. Das, A. Genovese, E. Di Fabrizio, and A. Diaspro: *J. Phys. Chem. C*, 115, (2011) 5102.
- [18] V. Švrček: *J. Laser Micro Nanoeng.*, 2, (2007) 15.
- [19] R. Intartaglia, K. Bagga, M. Scotto, A. Diaspro, and F. Brandi: *Opt. Mater. Express*, 2, (2012) 510.
- [20] E. Fazio, F. Barreca, S. Spadaro, G. Currò, and F. Neri: *Mater. Chem. Phys.*, 130, (2011) 418.
- [21] P. G. Kuzmin, G. A. Shafeev, V. V. Bukin, S. V. Garnov, C. Farcau, R. Carles, B. Warot-Fontrose, V. Guieu, and G. Viau: *J. Phys. Chem. C*, 114, (2010) 15266.
- [22] R. Intartaglia, K. Bagga, A. Genovese, A. Athanassiou, R. Cingolani, A. Diaspro, and F. Brandi: *Phys. Chem. Chem. Phys.*, 14, (2012) 15406.
- [23] S. Zhu, Y. F. Lu, and M. H. Hong: *Appl. Phys. Lett.*, 79, (2001) 1396.
- [24] P. Chewchinda, T. Tsuge, H. Funakubo, O. Odawara, and H. Wada: *Jpn. J. Appl. Phys.*, 52, (2013) 025001.
- [25] R. K. Soni, L. F. Fonseca, O. Resto, M. Buzaianu, and S. Z. Weisz: *J. Lumin.*, 83-84, (1999) 187.
- [26] C. Meier, S. Lüttjohann, V. G. Kravets, H. Nienhaus, A. Lorke, and H. Wiggers: *Phys. E Low-dimensional Syst. Nanostructures*, 32, (2006) 155.
- [27] P. Mishra, and K. Jain: *Phys. Rev. B*, 64, (2001) 1.



- [28] X. L. Wu, G. G. Siu, S. Tong, X. N. Liu, F. Yan, S. S. Jiang, X. K. Zhang and D. Feng: Appl. Phys. Lett., 69, (1996) 523.
- [29] K. Abderrafi, R. G. Calzada, M. B. Gongalsky, I. Suárez, R. Abarques, V. S. Chirvony, V. Y. Timoshenko, R. Ibáñez, and J. P. Martínez-Pastor: J. Phys. Chem. C, 115, (2011) 5147.
- [30] I. Stenger, B. Gallas, B. Jusserand, S. Chenot, S. Fisson, and J. Rivory: Eur. Phys. J. Appl. Phys., 44, (2008) 51.
- [31] P. Blandin, K. A. Maximova, M. B. Gongalsky, J. F. Sanchez-Royo, V. S. Chirvony, M. Sentis, V. Y. Timoshenko, and A. V. Kabashin: J. Mater. Chem. B, 1, (2013) 2489.
- [32] K. Sasaki, and N. Takada: Pure Appl. Chem., 82, (2010) 1317.
- [33] T. Tsuji, Y. Tsuboi, N. Kitamura, and M. Tsuji: Appl. Surf. Sci., 229, (2004) 365.
- [34] P. Lo Nostro, and B. W. Ninham: Chem. Rev., 112, (2012) 2286.
- [35] P. C. Schmidt, A. Weiss, and T. P. Das: Phys. Rev. B, 19, (1979) 5525.
- [36] J. E. Otterstedt and D. A. Brandreth: "Small particles technology" (Plenum Press, New York, 1998) p.197.
- [37] T. Cosgrove: "Colloid science principles, methods, and applications" (John Wiley & Sons Ltd, West Sussex, 2010) p.48.
- [38] P. Metrangolo, F. Meyer, T. Pilati, G. Resnati, and G. Terraneo: Angew. Chem. Int. Ed. 47 (2008) 6114.
- [39] A. R. Voth, P. Khuu, K. Oishi, and P. S. Ho: Nature Chem. 1 (2009) 74.
- [40] A. Vanderkooy, and M. S. Taylor: J. Am. Chem. Soc. 137 (2015) 5080.
- [41] G. Berger, J. Soubhye, and F. Meyer: Polym. Chem. 6 (2015) 3559.

**Figure captions:**

Fig. 1. TEM images along with size distribution of the samples prepared in (a) 2 mM (b) 4 mM (c) 6 mM (d) 8 mM and (e) 10 mM of NaCl solution.

Fig. 2. EDS spectrum and its corresponding image of the sample prepared in NaCl solution.

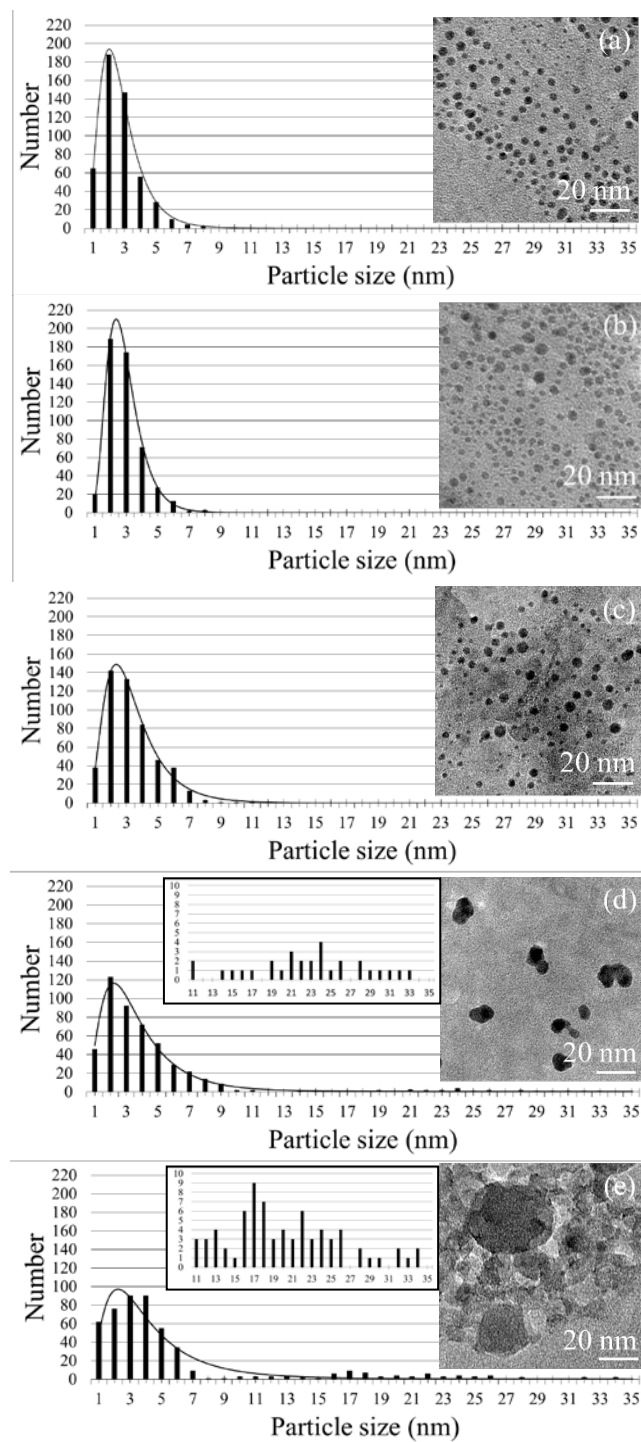
Fig. 3. TEM images along with size distribution of the samples prepared in (a) 2 mM (b) 4 mM (c) 6 mM (d) 8 mM and (e) 10 mM of NaBr solution.

Fig. 4. Raman spectra of the samples prepared in NaCl solution. Inset: HRTEM image of nanoparticles.

Fig. 5. Effect of electrolyte concentration and surface charge on electric double layer thickness.

**Table 1** Polarizability of ions [34-35]

Ions	Polarizability ( $\text{\AA}^3$ )
Na <sup>+</sup>	0.148
Cl <sup>-</sup>	3.420
Br <sup>-</sup>	4.850
I <sup>-</sup>	7.510



**Fig. 1** TEM images along with size distribution of the samples prepared in (a) 2 mM (b) 4 mM (c) 6 mM (d) 8 mM and (e) 10 mM of NaCl solution.

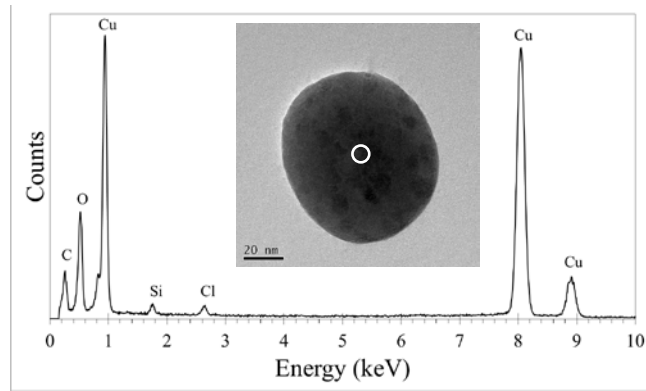


**Fig. 2** EDS spectrum and its corresponding image of the sample prepared in NaCl solution.

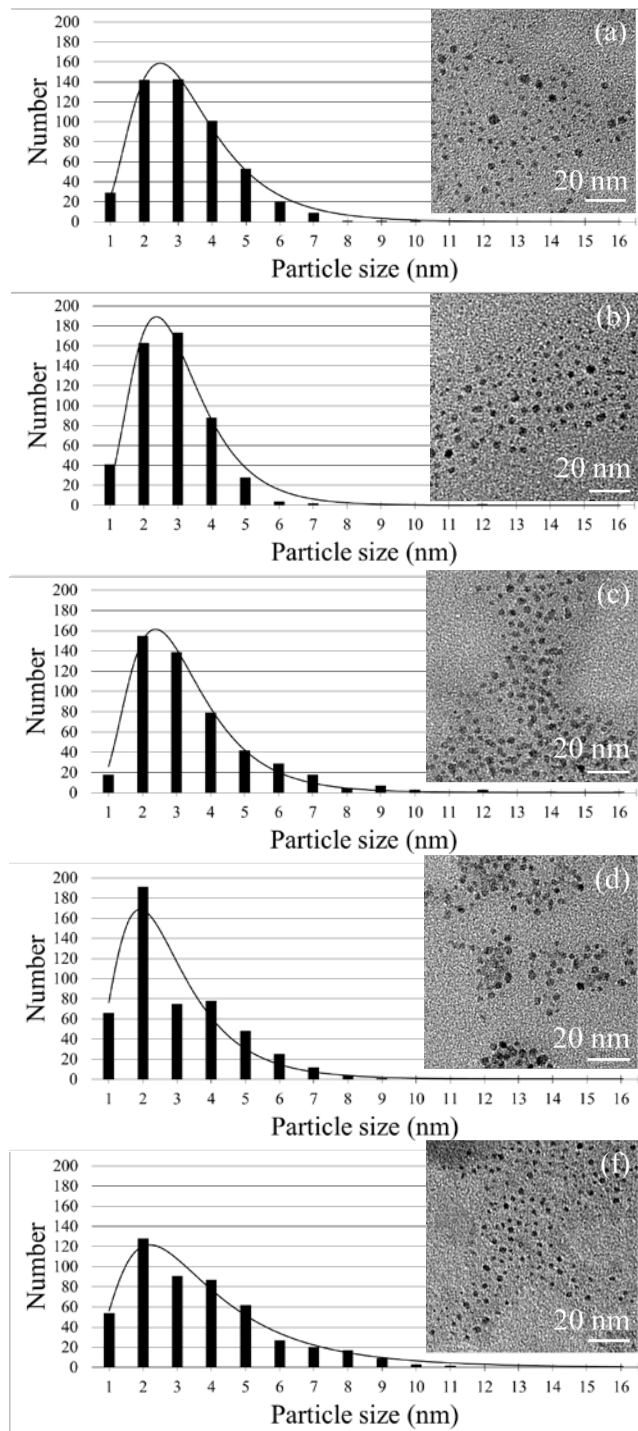


**Fig. 3** TEM images along with size distribution of the samples prepare in (a) 2 mM (b) 4 mM (c) 6 mM (d) 8 mM and (e) 10 mM of NaBr solution.

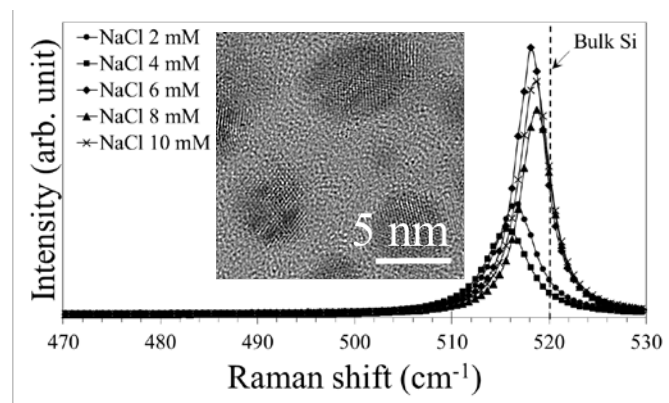


**Fig. 4** Raman spectra of the samples prepared in NaCl solution.  
Inset: high resolution TEM image of nanoparticles.

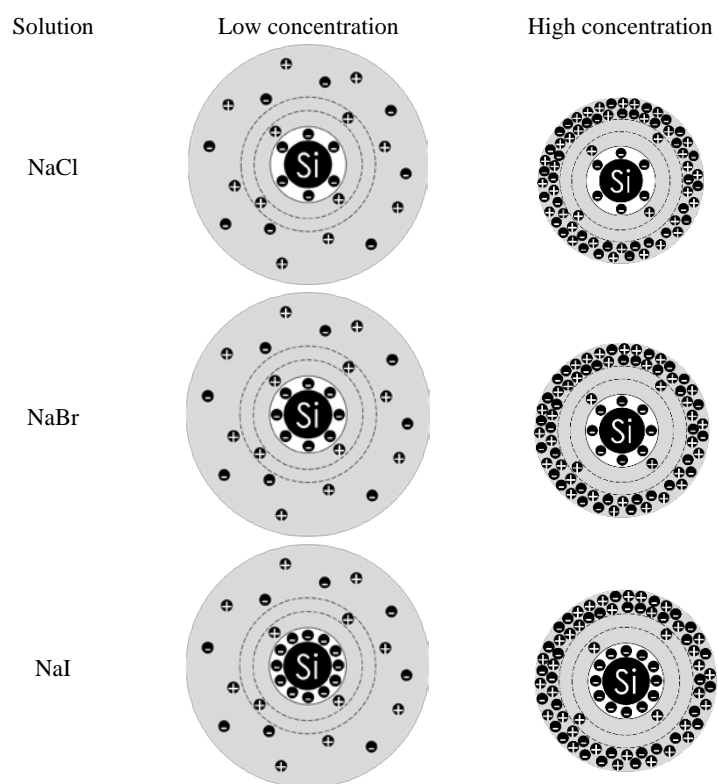
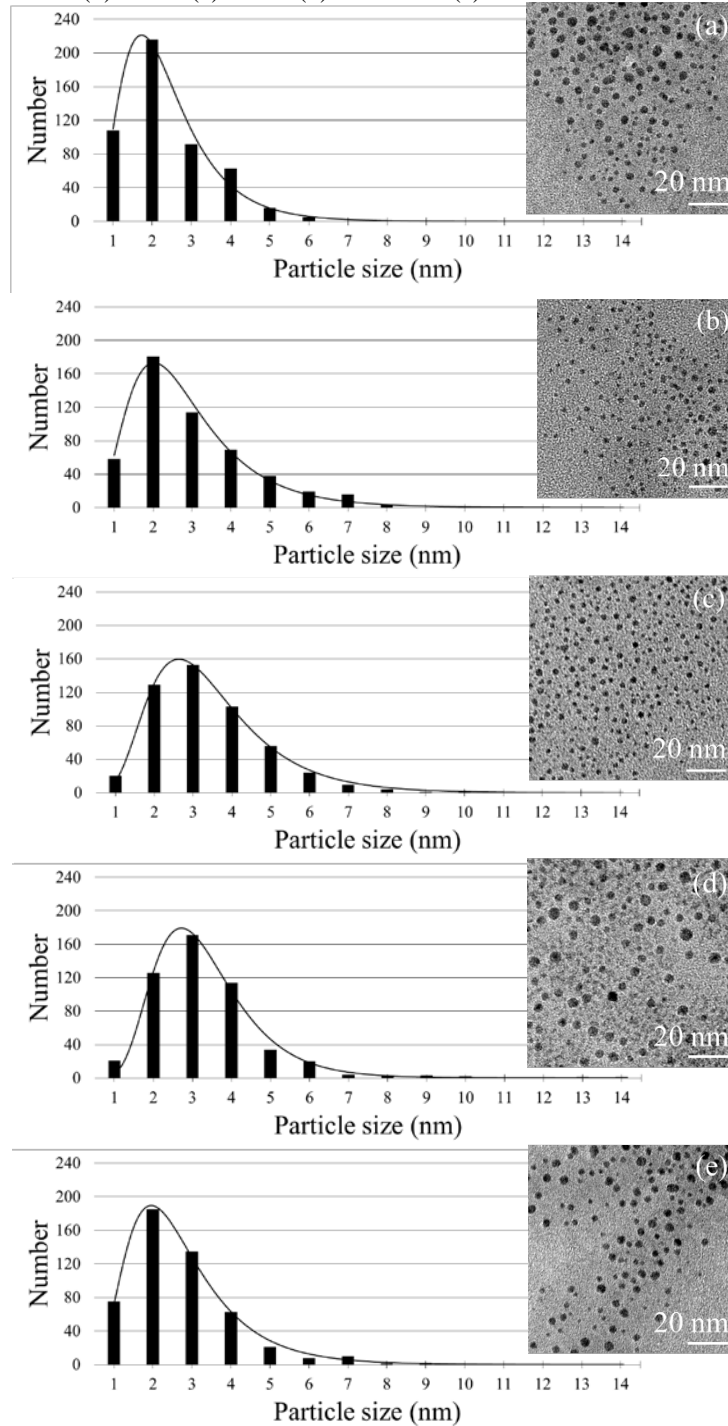


**Fig. 5** Effect of electrolyte concentration and surface charge on electric double layer thickness.



### Appendix A

TEM images along with size distribution of the samples prepared in (a) 2 mM (b) 4 mM (c) 6 mM (d) 8 mM and (e) 10 mM of NaI solution.



### Appendix B

Raman spectra of the samples prepared in (a) NaBr and (b) NaI solution.

